F2012-A04-031

THE APPLICATION OF NANOMETRIC COMPOSITE MATERIALS IN A DIESEL ENGINE IN THE ASPECT OF IMPROVEMENT OF DEEP BED FILTRATION IN A DIESEL PARTICULATE FILTER

[1]Merkisz Jerzy; [1]Fuc Pawel[*]; [1]Lijewski Piotr; [1]Ziolkowski Andrzej
[1]Poznan University of Technology, Poland

KEYWORDS – particulate matter, diesel particulate filter, research under real operating conditions

ABSTRACT – The question of Diesel Particulate filter regeneration, despite many years of research, is still an existing problem. Currently, at the expense of the filter durability, the rate of variation of the thermodynamic parameters is increased in the exhaust systems in order to burn the particulate matter accumulated in the DPF filter. This is particularly the case for filters fitted in passenger vehicles operated in the urban cycle [1, 3, 7].
During the analysis the authors took into account the synergy of the aftertreatment components and the physical and chemical phenomena occurring in the integrated co-dependent aftertreatment systems in a diesel engine. The paper includes an analysis and results of tests performed under actual traffic conditions on vehicles fitted with modern aftertreatment systems [4-6]. In the performed tests stress was put on finding the possibility of improving of the DPF deep bed filtration through analysis of PM emission and size distribution. The considered area of investigations has been defined using nanometric composite materials based on highly porous supports of materials that are at the same time ionic conductors. For the research unique equipment has been used for tests under actual traffic conditions, which enabled a full analysis of the interactions of the gaseous emissions and particulate matter. An analysis of the PM size distribution and PM number has been performed during operation under actual traffic conditions.

INTRODUCTION

The most frequently used diesel particulate filter supports are cordierite supports, yet their durability and efficiency, particularly at longer periods of operation is limited. The basic problem is the increased flow resistance resulting from the clogging of the porous material, formation of ash in the interchangeably blanked cells of the support and material fracture resulting from various physical and chemical parameters of the filtering and/or blanking parts. Another limitation is the chemical processing in the aspect of formation of the active layer due to a lack of chemical activity of highly sintered cordierite (does not react with typical reducers and does not provide good conditions for low temperature catalyst application). In the case of SiC supports the problem is the low microporousness after the production process, which forces additional processing of chemical etching (hydrofluoric acid) or microsurface reduction with hydrogen to develop the surface. Classic SiC supports have low resistance to fracture resulting from the physical and chemical properties of the $SiC\text{-}SiO_2$ composite. Their advantages however are high thermal conductivity, high resistance to abrasion, resistance to breakability as well as resistance to chemical and gas induced corrosion. These advantages make the application of this SiC support in the atmosphere of exhaust gases purposeful from the point of view of its high efficiency in extended periods of operation. A significant elimination of the disadvantages of the classic SiC support forces the development of composite materials and parameters of the production process of the washcoat.

THE OBTAINMENT OF TIO_2-RUO_2- COMPOSITE NANOSPHERES THROUGH THE FSP METHOD

An example of a synthesis of the nanometric catalytic composite was the synthesis of the solid solution in TiO_2-RuO_2 system [2] Isostructural oxides of TiO_2-RuO_2 of very good mixing properties in the nanospheres were obtained through the FSP method. The base products for the synthesis of the solid solution in TiO_2-RuO_2 system were isopropyl titanium alkoxide 97% developed by Aldrich and ruthenium chloride 0,01M $RuCl_3$ in the solution of ethanol.
The highest temperature range in which the sublayer of TiO_2 and the RuO_2 catalysts were in the flame zone was 860-900^oC in the H_2:O_2 , ratio 1:1. The carrier gas in this case was argon with 4% hydrogen.
In the FSP synthesis process nanometric bimodal spheres were obtained (two ranges of grain) of the powders, with the prevailing grain size of below 100 nm.
Figure 1 presents the image of the colony of the RuO_2-TiO_2 nanospheres with a clearly shown nanopsherical build. Figure 2 shows the distribution of Ti and Ru within the sphere.

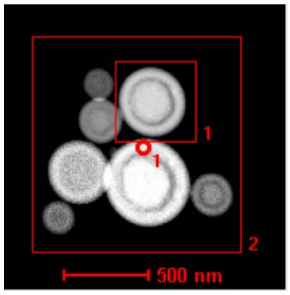

Fig. 1. HRTEM morphology of the TiO_2-RuO_2 colony **Błąd! Nie można odnaleźć źródła odwołania.**

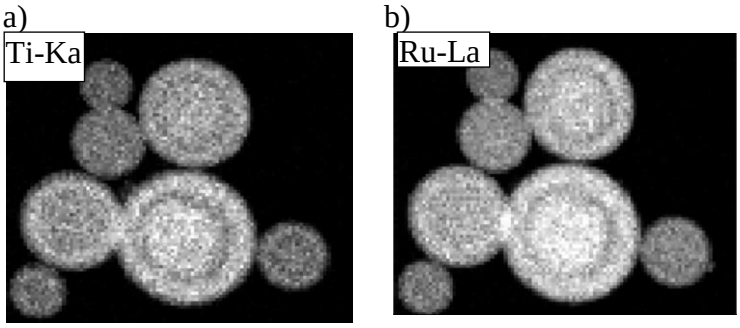

Fig. 2. HRTEM morphology of the TiO_2-RuO_2 colony showing the distribution of: a) Ti-Ka; b) Ru-La respectively **Błąd! Nie można odnaleźć źródła odwołania.**

Figure 3 presents the linear analysis of the distribution of atoms of Ti and Ru on the surface of the sphere of the diameter of 160 nm. In the solid solution of TiO_2-RuO_2 on the surface of the sphere, the crystals of RuO_2 are mixed 1:1 with the crystals of TiO_2 and form crystal structures of the solid solution in which titanium (on the atomic level) in the nano crystal structure blocks the thermal dissociation of ruthenium in the oxygen atmosphere. Figure 4 in the range of 5 nm presents the area of edge defects of the TiO_2-RuO_2 sphere obtained through the FSP method. The TiO_2-RuO_2 forming the external nanosphere layer allows good anchoring of the catalyst on the surface. Numerous edge defects occurring in the TiO_2-RuO_2 sphere suggest that the TiO_2-RuO_2 catalytic nanopowders obtained through FSP have an elevated proneness to form donors triggering the activation of oxygen.

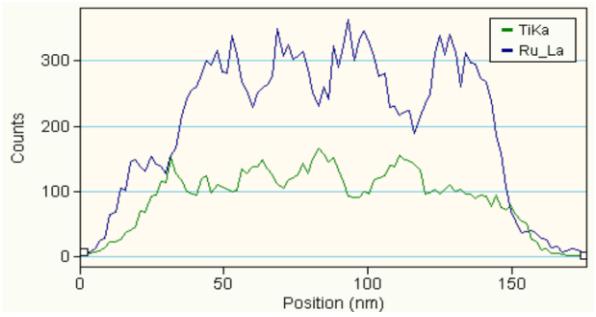

Fig. 3. Linear analysis of the distribution of Ti and Ru on the surface of the sphere of the diameter of 160 nm

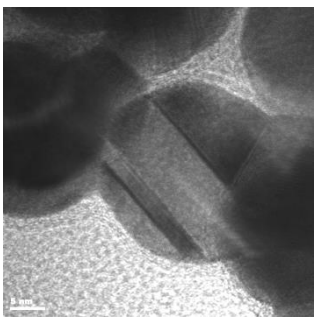

Fig. 4. HRTEM image of the edge defect of the TiO_2 -RuO_2 sphere obtained through

the FSP method

EXPERIMENTAL RESEARCH ON THE CATALYTIC MATERIALS

Normative and short time simulations of the road conditions corresponding to selected driving cycles under different engine operating conditions (temperature, engine load, exhaust emissions) allow a simultaneous analysis of the exhaust components and particulate matter (PM). The values obtained from the latest technology measurements of the DOC catalyst and the DPF filter assembly (the structural part and the oxidation part) of own design and make can be compared to the values obtained in the measurements of the parameters of the OEM DPF filter. In the measurement system an oval DPF filter was used of the dimensions of 130x150x245 mm manufactured by a French manufacturer. The filter was of the volume of 2,8 dm^3. The tested catalytic system of the filter (the DOC part) was of the volume of 0,7 dm^3, while the filter itself was of the volume of 2,1 dm^3. The filter channels were of the size of 100 cpsi.
For the test a catalyst was selected (as a substitute for commercial Pt catalyst) – of the nanosphere composition: TiO_2-0,1RuO_2-0,15 PdO_2. The catalyst was applied on seven SiC discs, surface modified with the Ti_4O_7 nanospheres of the size of 100 mm and the thickness of 20 mm. Such a design of the test system allowed a volume of 1,1 dm^3. In the test a complex analysis of the possibilities of obtaining of composite, highly porous surface modified and fully modified sinters with such additives as: TiO_2, Al_2TiO_5, $MgAl_4Si_5O_{18}$. The assumptions were based on the results of complex investigations, some results of which have been shown in table 1.

Tab. 1.Basic parameters of the tested catalytic supports

Material/ parameter	Cordierite	SiC	Al_2SiO_5	Ti_4O_7
Thermal expansion coefficient α x 10^{-7}/ C	3-7	4-4,5	9	9
Melting point T_t [ºC]	1460	2400	1600	1860
Thermal conductivity coefficient γ[W/m*K]	1	20	1	11,9- 30
Thermal capacity [J/g*C]	0,51	0,95	0,65	0,75
Resistance to thermal shocks T=25-800º C t=1000 cycles	+	+/-	+	+
Specific mass [g/cm3]	2,5	3,24	3,4	3,68
Young modulus E[GPa]	4,7	33,3	8,3	9,1
Porosity [%]	50-80	40-60	50-80	50-70
Size of pores [μm]	10-20	10-20	10-20	10-20
Average size of pores [μm]	-	10-12	15-18	14-17
Open porosity (mercury) [%]	-	49-51	45-65	40-60
Density of the channel cells [cells/ mm^2]	200	0,35	0,465	80
Thickness of walls [mm]	0,15	0,25	0,33	0,29

Nanotechnologically formed spheres (FSP method) such as Ti_4O_7 were used for the formation of sponge-like discs of the diameter of 100 mm, thickness 20 mm, porosity 80% and pore size 80 ppi. Based on the nano intermetallic alloy technology and the production of self-supported highly porous DOC a series of catalytically active Pd-Ag, NiAl and Pd_3Ni sponge-like sinters were made.

TEST BED INVESTIGATIONS

Based on extensive data obtained in the urban and extra urban driving cycles verification test were performed on the engine test bed simulating the extra urban driving in order to answer

the question of what the time is of the filter response to the engine parameters. The results obtained for the commercial filter and the tested material have been presented in table 2.

Tab. 2. Tests on the commercial and experimental filters under engine test bed conditions at selected engine operating parameters

Filter material	Background				SiC commercial filter				Tested material -1/4 of the volume of the commercial filter			
Engine speed [rpm]	2000				2000				2000			
Load [Nm]	0	40	60	80	0	40	60	80	0	40	60	80
Collective concentration– number of PM of different diameters - EEPS [l. cz./s] x1000	1426841	2907019	11132702	7300540	4399115	1018299	5590240	1704905	2376128	1531791	4257921	6238321
Filtering efficiency [%]	-				30	35	50	23	16	5,2	38	8,5

Figures 5 present the characteristics of the obtained PM emissions: PM number and PM average size distribution for the engine speed n=2000 rpm and the engine load M=60 Nm. The nature of the two curves shown in the first graph indicates a normal distribution. The first curve (dark green) shows the number of particles emitted for the engine operating conditions without a filter. For this curve we ca see a maximum at the point 43,3 i.e. for the average PM sizes of 43,3 nm. The other curve (light green) shows the number of PM emitted for the engine operating conditions with a filter. For this curve we can see a maximum at the point of 60,4 i.e. for the average PM sizes of 60,4 nm. The shift of the curve showing the number of PM emitted for the system with a filter against the curve showing the operation without a filter is in line with the assumption that as the flow resistance grows, the number of collisions among the soot particles as well as between the soot particles and the walls increases, which leads to joining of the nanoparticles into aggregates.

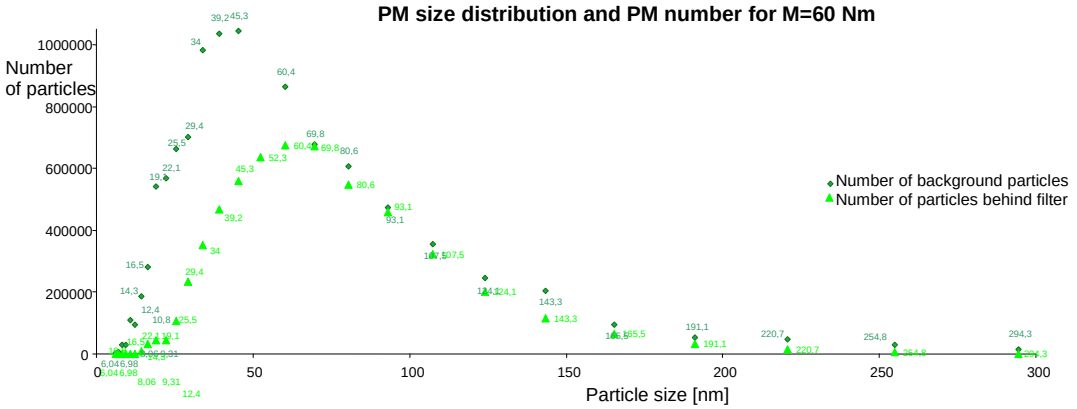

Fig. 5. PM size distribution and PM number at the engine load M=60 Nm and engine speed n=2000 rpm

TESTS ON THE COMMERCIAL PM FILTERS IN THE CITY TRAFFIC UNDER ACTUAL DRIVING CONDITIONS

The filter efficiency tests were carried out under actual traffic conditions in order to compare the urban and extra urban driving cycles for which DPF filter regeneration may be triggered. The tests were carried out in the urban cycle on the route lengths:

1. Vehicle A – S=11,96 km; V_a=37 km/h – technical specifications – table 3.
2. Vehicle B – S=10,3 km; V_a=19 km/h – technical specifications – table 4.

Tab. 3. Selected engine and vehicle parameters used for the tests of vehicle A

Displacement	Maximum power	Maximum torque
1896 cm³	170 KM (125 KW) at 4000 rpm	350 Nm at 1800 rpm

Tab.4. Selected engine and vehicle parameters used for the tests of vehicle B

Displacement	Maximum power	Maximum torque
1896 cm³	115 KM (85 KW) at 4000 rpm	285 Nm at 1900 rpm

a) b)

Fig. 6. Route distances during urban traffic tests: a) S=10,9 km; b) S=11,2 km

Figure 6 shows the routes that were used for the city traffic tests. The routes were chosen because of their length and characteristics. Because vehicles have to undergo homologation tests the routes were selected (their characteristics) so that the NEDC homologation conditions were reflected. This test as said earlier is composed of the urban and extra urban part. Each of these parts has different maximum driving speeds (52 km/h and 120 km/h). That is why the routes (Fig. 6 a, b) for the tests in the urban cycle under actual operating conditions were selected to simulate both parts of the NEDC test. In order to better picture the conditions of urban operation the selected routes were divided into two groups:
I urban driving – vehicle A – time span t=1181 s – t=19, 6 min. with average speed – V_a=37 km/h – referred to as vehicle A (Fig. 6b),
II urban driving – vehicle B – time span t=1181s=19, 6 min. with average speed – V_a=19 km/h – referred to as vehicle B (Fig. 6a).
Range I – vehicle A:
- minimum vehicle speed V=0 km/h,
- maximum vehicle speed V=112 km/h,
- minimum engine load M=0%,
- maximum engine load M=98%,
- driving time – t= 19,6 min.

The maximum concentration of NO_2 in the driving cycle for range I was 252,8 ppm – determined for the measuring time of 304 s and the minimum value of the NO_2 concentration in the driving cycle for this same range was 60 ppm determined for the measuring time of 918 s (Fig. 7).
When analyzing the first range the vehicle speed was within 0–112 km/h (for measurements made from t=21–785th second of the test). Lack of velocity occurred for 93 s, which constituted 8% of the whole driving cycle. The minimum engine load M=0% (idle) occurred for the measurement made in time t=116 s, which constituted 10% of the whole driving cycle. The maximum engine load M=99% occurred for the measurement made in time t=748 s.

Literature analysis and own research experience indicate that the soot deposited on the filter walls in the amount of 45% of the total filter volume results in a deactivation of the EGR allowing an additional fuel injection in the exhaust stroke (post-injection). This process allows the exhaust gases in the exhaust system to reach the temperature of T=600ºC, which is sufficient to trigger the soot afterburn. Such a state, however, is difficult to obtain under the conditions of start/stop driving, which is prevalent in the urban cycle. In such a case and in the case of vehicle driving with relatively low speeds the regeneration process is interrupted or does not initiate at all.
The graph of the particulate matter distribution (Fig. 8) shows that for the measurement range of vehicle A in the urban cycle the dominant particles are the ones of the size of 10,8 nm otherwise referred to as ultrafine – <1 μm.

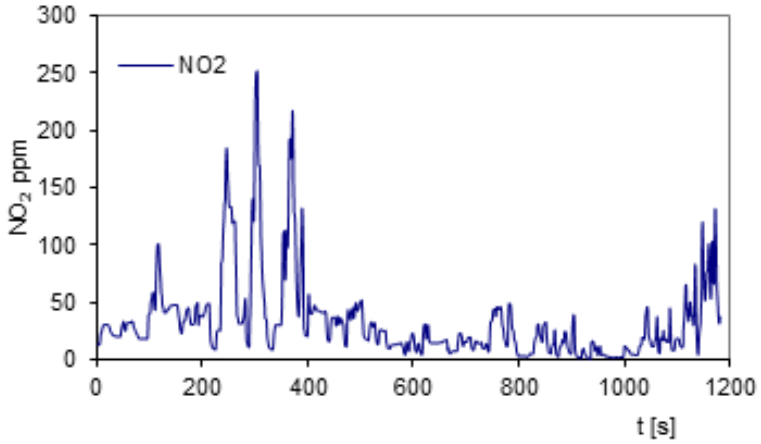

Fig. 7. Dependence of the NO_2 concentration as a function of time for the tests under the conditions of actual operation for the urban cycle – vehicle A

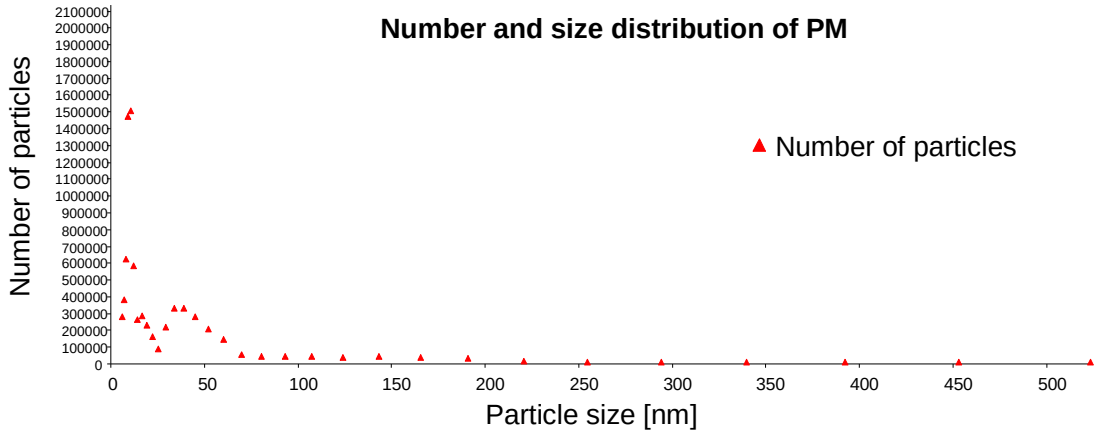

Fig. 8. Number and size distribution of PM under the conditions of actual operation for the urban cycle – vehicle A

Range II – vehicle B:
- minimum vehicle speed V=0 km/h,
- maximum vehicle speed V=69 km/h,
- minimum engine load M=0%,
- maximum engine load M=99%,
- driving time – t=19,6 min.

The maximum concentration of NO_2 in the cycle (vehicle B) was 260 ppm – determined for the measuring time of t=733 s and the minimum concentration of NO_2 in the driving cycle for this same range was 7 ppm determined for the measuring time t=835 s (Fig. 9). The vehicle

speed was recorded in the range of 0–66 km/h (for the measurements made in the 1st and 831th second respectively). Lack of velocity occurred for t=234 s, which constituted 20% of the whole driving cycle. The minimum engine load M=0% – (idle) occurred for t=11 s, which constituted 1% of the whole driving cycle. The maximum engine load M=99% was observed for the measurement made in time t=724 s. The whole route of the urban cycle for vehicle B was in the mixed mode. For the performed analysis it results that the vehicle speed of V > 60 km/h constituted 6% of the whole urban driving cycle. In this cycle there was no road portion on which the vehicle would drive with the speed of V > 60 km/h for at least 10 min.
The concentration of NO_2 indicates that in t=225–819 s there were numerous maximums. In the time span t=594 s, the vehicle speed was higher than V > 40 km/h in time t=45 s, which constitutes 8% of the whole measurement road portion where the NO_2 maximums are visible. The NO_2 concentration maximums appeared many times in a single time span. The maximum NO_2 concentrations are for the measuring points: t=603 s – NO_2=255 ppm and t=733s – NO_2=259 ppm. The analysis of speed V and load M has shown that the engine worked at idle 7 times and there were 4 stops of the vehicle preceding the maximum NO_2 emissions. The total concentration of NO_2 in the whole measurement range t=1181 s in the cycle of vehicle B was 80 999,69 ppm NO_2 and was twice as high as the total concentration of NO_2 in the cycle of vehicle A– 38 805 ppm NO_2. The total time in which the vehicle operated at the speed of V=60 km/h was 74 s. This time was insufficient to provide the thermal conditions for the regeneration process.
The graph of the distribution of the PM number (Fig. 10) shows that for the cycle of vehicle B (similarly to vehicle A) the dominant particles are the ones of the size of 10,8 nm otherwise referred to as ultrafine – <1 μm.

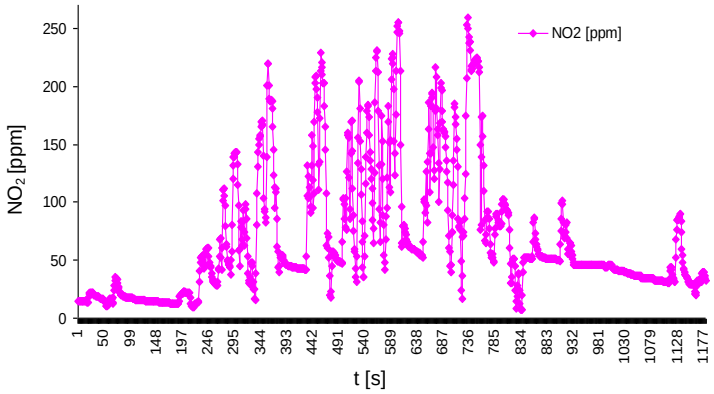

Fig. 9. The concentration of NO_2 under the conditions of actual city traffic operation marked as vehicle B

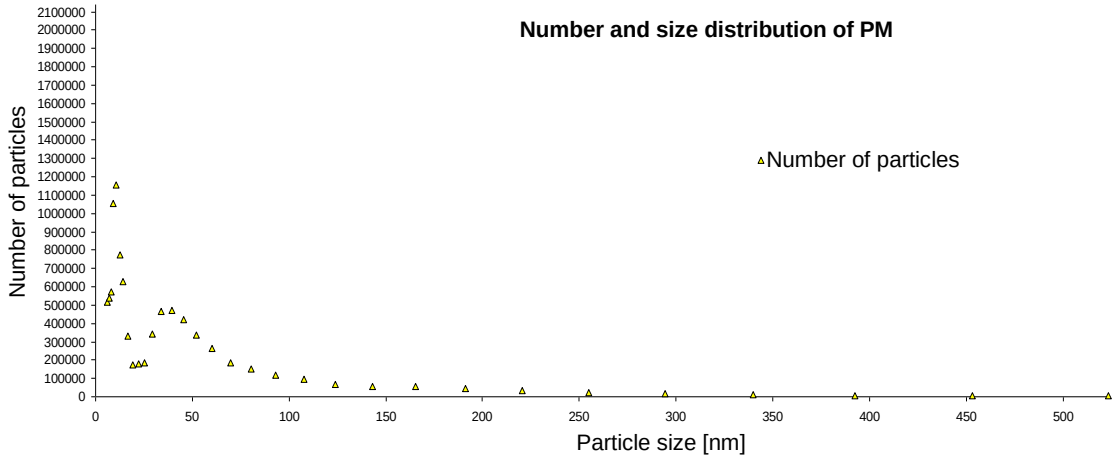

Fig. 10. PM number and size distribution under the conditions of actual city traffic operation marked as vehicle B

CONCLUSIONS

1. The research possibilities in nanoscale (TEM microscopy/HRTEM - high resolution TEM microscopy) allowed making assumptions for the production of materials based on nano structures (both single and multi component) of repeat composition, structure, size, physical and chemical properties.
2. The modification of many unwanted features was realized through melting in of the Ti_4O_7 nanospheres between the SiC grains and the covering SiO_2 enamel. This consisted in: an increased resistance of the material to fracture, an increase of the resistance to thermal shocks, a reduction of the thermal conductivity, an obtainment of better surface development, an increase of the microporosity of the sinter, an extension of the time of operation (even in the case of frequent regeneration cycles) and better activity.
3. The sponge-like sinters, obtained during the research from the Ti_4O_7 spheres and the Pd/Ag alloys showed high resistance to fracture and in the case of the sinters obtained from the Pd/Ag additional higher catalytic activity was observed, which provides new potential for use of novel material of improved functional parameters by the automotive industry.
4. Statistical research carried out on the engine test bed as well as dynamic tests carried out based on the developed methodology of NEDC test simulation under actual operating conditions allowed a verification of the possibilities in the aspect of preliminary, comparative and criteria-based research.
5. The tests performed under actual operating conditions have shown the dynamics of the changes of the operating parameters and engine conditions and its influence on the functional parameters of the aftertreatment system i.e. catalytic converter (exhaust gases) and DPF filter (soot and ash).
6. The engines for the laboratory research and the vehicles for the on-road tests were carefully chosen. This allowed a verification of the parameters of the filtering devices under a variety of conditions and a development of the assumptions for the procedure of filter regeneration.

REFERENCES

1. Czerwiński J., Comte P., Reutimann A., Mayer A.: Influence of (hydrous) ethanol blends on (particle) emissions of small 2-& 4-stroke scooters – Part 1. Combustion Engines 1/2011.
2. Fuć P., Non Pt catalyst group in active part of new PM filter. SAE International Congress, 2008-01-1551 Shanghai 2008.
3. Gao Y., Checkel M.D.: Emission Factors Analysis for Multiple Vehicles Using an On-Board, In-Use Emissions Measurement System. SAE Technical Paper Series 2007-01-1327.
4. Merkisz J., Fuc P.: The Exhaust Emission from Light Duty Vehicles in Road Test in Urban Traffic. International Powertrains, Fuels & Lubricants Meeting, May 2010, Rio De Janeiro, Brazil, 2010. SAE Paper 2010-01-1558.
5. Merkisz J., Lijewski P., Fuc P., Pielecha J.: Exhaust emission tests from agricultural machinery under real operating conditions. SAE 2010 Commercial Vehicle Engineering Congress, October, 2010, Chicago, IL, USA, 2010. SAE Paper 2010-01-1949.
6. Merkisz J., Fuc P., Lijewski P.: The on-road operation of diesel particulate filter. Combustion Engines 3/2011.
7. Zaigrayew L., Shekhovtsov Y., Ignatov.: Research into particulate filter passive regeneration under operating conditions. Combustion Engines 4/2011.